



## 22 Introduction

23 The advent of affordable next-generation sequencing and SNP-typing assays allows large num-  
24 bers of polymorphic genetic markers to be characterised in almost any system. A common chal-  
25 lenge is how to organise these genetic variants into a coherent order for downstream analyses,  
26 as many approaches rely on marker order information to gain insight into genetic architectures  
27 and evolutionary processes (Ellegren, 2014). Linkage maps are often an early step in this pro-  
28 cess, using information on recombination fractions between markers to group and order them  
29 on their respective chromosomes (Sturtevant, 1913; Lander & Schork, 1994). Ordered mark-  
30 ers have numerous applications, including: trait mapping through quantitative trait locus (QTL)  
31 mapping, genome-wide association studies (GWAS) and regional heritability analysis (Bérénos  
32 *et al.*, 2015; Fountain *et al.*, 2016); genome-scans for signatures of selection and population  
33 divergence (Bradbury *et al.*, 2013; McKinney *et al.*, 2016); quantification of genomic inbreeding  
34 through runs of homozygosity (Kardos *et al.*, 2016); investigation of contemporary recombi-  
35 nation landscapes (Kawakami *et al.*, 2014; Johnston *et al.*, 2016); and comparative genomics  
36 and genome evolution (Brieuc *et al.*, 2014; Leitwein *et al.*, 2016). Linkage maps also provide  
37 an important resource in *de novo* genome assembly, as they provide information for anchoring  
38 sequence scaffolds and allow prediction of gene locations relative to better annotated species  
39 (Fierst, 2015).

40 Nevertheless, creating linkage maps of many thousands of genome-wide markers *de novo* is  
41 a computationally intensive process requiring pedigree information, sufficient marker densities  
42 over all chromosomes and billions of locus comparisons. Furthermore, the ability to create a  
43 high resolution map is limited by the number of meioses in the dataset; as marker densities  
44 increase, more individuals are required to resolve genetic distances between closely linked  
45 loci (Kawakami *et al.*, 2014). Whilst *de novo* linkage map assembly with large numbers of  
46 SNPs is possible (Rastas *et al.*, 2016), one approach to ameliorate the computational cost and  
47 map resolution is to use genome sequence data from related species to inform initial marker  
48 orders. Larger and finer scale rearrangements can then be refined through further investigation  
49 of recombination fractions between markers.

50 In this study, we use this approach to construct a high density linkage map in a wild population  
51 of red deer (*Cervus elaphus*). The red deer is a large deer species widely distributed across

52 the northern hemisphere, and is a model system for sexual selection (Kruuk *et al.*, 2002), be-  
53 haviour (Clutton-Brock *et al.*, 1982), hybridisation (Senn & Pemberton, 2009), inbreeding (Huis-  
54 man *et al.*, 2016) and population management (Frantz *et al.*, 2006). They are also an increas-  
55 ingly important economic species farmed for venison, antler velvet products and trophy hunting  
56 (Brauning *et al.*, 2015). A medium density map (~ 600 markers) is available for this species,  
57 constructed using microsatellite, RFLP and allozyme markers in a red deer × Père David's  
58 deer (*Elaphurus davidianus*) F<sub>2</sub> cross (Slate *et al.*, 2002). However, these markers have been  
59 largely superseded by the development of the Cervine Illumina BeadChip which characterises  
60 50K SNPs throughout the genome (Brauning *et al.*, 2015). Estimated SNP positions are known  
61 relative to the cattle genome, but the precise order of SNPs in red deer remains unknown. Here,  
62 we integrate pedigree and SNP data from a long-term study of wild red deer on the island of  
63 Rum, Scotland to construct a predicted linkage map of ~ 38,000 SNP markers and a skele-  
64 ton linkage map of ~11,000 SNP markers. As well as identifying strong concordance with the  
65 cattle genome and several chromosomal rearrangements, we also present evidence of strong  
66 sexual dimorphism in recombination rates (i.e. heterochiasmy) at centromeric regions of the  
67 genome. We discuss the implications of our findings for other linkage mapping studies and  
68 potential drivers of recombination rate variation and heterochiasmy within this system.

## 69 **Materials and Methods**

### 70 **Study Population and SNP dataset.**

71 The red deer population is located in the North Block of the Isle of Rum, Scotland (57°02'N,  
72 6°20'W) and has been subject to an on-going individual-based study since 1971 (Clutton-Brock  
73 *et al.*, 1982). Research was conducted following approval of the University of Edinburgh's An-  
74 imal Welfare and Ethical Review Body and under appropriate UK Home Office licenses. DNA  
75 was extracted from neonatal ear punches, post-mortem tissue, and cast antlers (see Huisman  
76 *et al.*, 2016 for full details). DNA samples from 2880 individuals were genotyped at 50,541  
77 SNP loci on the Cervine Illumina BeadChip (Brauning *et al.*, 2015) using an Illumina genotyp-  
78 ing platform (Illumina Inc., San Diego, CA, USA). SNP genotypes were scored using Illumina  
79 GenomeStudio software, and quality control was carried out using the *check.marker* function in  
80 GenABEL v1.8-0 (Aulchenko *et al.*, 2007) in R v3.3.2, with the following thresholds: SNP geno-

81 typing success >0.99, SNP minor allele frequency >0.01, and ID genotyping success >0.99.  
82 A total of 38,541 SNPs and 2,631 IDs were retained. The function identified 126 pseudoau-  
83 toosomal SNPs; heterozygous genotypes at non-pseudoautosomal X-linked SNPs within males  
84 were scored as missing. A pedigree was constructed in the software Sequoia (Huisman, 2017;  
85 see Huisman *et al.*, 2016 for information on deer pedigree construction).

## 86 **Linkage map construction.**

87 A standardised sub-pedigree approach was used for linkage map construction (Johnston *et al.*,  
88 2016). The pedigree was split as follows: for each focal individual (FID) and its offspring, a  
89 sub-pedigree was constructed that included the FID, its parents, the offspring, and the other  
90 parent of the offspring (Figure 1), and were retained where all five individuals were SNP  
91 genotyped. This pedigree structure characterises crossovers occurring in the gamete trans-  
92 ferred from the FID to the offspring. A total of 1355 sub-pedigrees were constructed, allow-  
93 ing characterisation of crossovers in gametes transmitted to 488 offspring from 83 unique  
94 males and 867 offspring from 259 unique females. Linkage mapping was conducted using  
95 an iterative approach using the software CRI-MAP v2.504a (Green *et al.*, 1990), with input  
96 and output processing carried out using the R package *crimaptools* v0.1 (S.E.J., available  
97 <https://github.com/susjoh/crimaptools>) implemented in R v3.3.2. In all cases, marker order was  
98 specified in CRI-MAP based on the criteria outlined in each section below. Code for the deer  
99 map construction is archived at <https://github.com/susjoh/DeerMapv4>.

100 **Build 1: Order deer SNPs based on synteny with cattle genome.** Mendelian incompati-  
101 bilities were identified using the CRI-MAP *prepare* function, and incompatible genotypes were  
102 removed from both parents and offspring. SNPs with Mendelian error rates of >0.01 were dis-  
103 carded (N = 0 SNPs). Sub-pedigrees with more than 50 Mendelian errors between an FID  
104 and its offspring were also discarded (N = 4). All SNPs were named based on direct synteny  
105 with the cattle genome (BTA vUMD 3.0; N = 30), and so loci were ordered and assigned to  
106 linkage groups assuming the cattle order and a sex-averaged map of each chromosome was  
107 constructed using the CRI-MAP *chrompic* function (N = 38,261 SNPs, Figure S1).

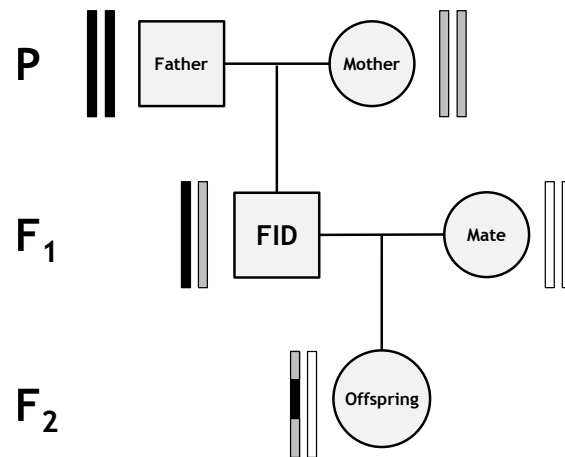


**Figure 1:** Sub-pedigree structure used to construct linkage maps. Rectangle pairs next to each individual represent chromatids, with black and grey shading indicating chromosome or chromosome sections of FID paternal and FID maternal origin, respectively. White shading indicates chromatids for which the origin of SNPs cannot be determined. Crossovers in the gamete transferred from the focal individual (FID) to its offspring (indicated by the grey arrow) can be distinguished at the points where origin of alleles origin flips from FID paternal to FID maternal and vice versa. From (Johnston *et al.*, 2016).

108 **Build 2: Rerun cattle order with wrongly positioned chunks removed.** All SNP loci from  
109 Build 1 were assigned to “chunks”, defined as a run of SNPs flanked by map distances of  $\geq 3$   
110 centiMorgans (cM). Several short chunks were flanked by large map distances, indicating that  
111 they were wrongly positioned in Build 1 (Figure S1); chunks containing  $<20$  SNPs were removed  
112 from the analysis for Build 2 (N = 327 SNPs). A sex-averaged map of each chromosome was  
113 reconstructed using the *chrompic* function (N = 37,934 SNPs, Figure S2).

114 **Build 3: Arrange chunks into deer linkage groups.** SNPs from Build 2 were arranged into  
115 34 deer linkage groups (hereafter prefixed with CEL) based on a previous characterisation of  
116 fissions and fusions from the red deer  $\times$  Père David’s deer linkage map (Slate *et al.*, 2002)  
117 and visual inspection of linkage disequilibrium (LD,  $R^2$ , calculated using the *r2fast* function in  
118 GenABEL; Figure S3). There was strong conformity with fissions and fusions identified in the  
119 previous deer map (Table 1); intra-marker distances of  $\sim 100$  cM between long chunks indicated  
120 that they segregated as independent chromosomes. In Build 2, chunks flanked by gaps of  $\ll$   
121 100cM but  $>10$ cM were observed on the maps associated with BTA13 (CEL23) and BTA28  
122 (CEL15; Figure S2). Visual inspection of LD indicated that these chunks were incorrectly orien-  
123 tated segments of  $\sim 10.5$  and  $\sim 24.9$  cM in length, respectively (Figure S3a and S3b; Table 1).  
124 Reversal of marker orders in these regions resulted in map length reductions of 19.4 cM and  
125 20.9 cM, respectively. Visual inspection of LD also confirmed fission of CEL19 and CEL31 (syn-

126 tenic to BTA1), with a 45.4cM inversion on CEL19 (Figure S3c). The X chromosome (BTA30,  
127 CEL34) in Build 2 was more fragmented, comprising 9 chunks (Figure S4). Visual inspection of  
128 LD in females indicated that chunks 3 and 7 occurred at the end of the chromosome, and that  
129 chunks 4, 5 and 6 were wrongly-oriented (Figure S5). After rearrangement into new marker  
130 orders, a sex-averaged map of each deer linkage group was reconstructed using the *chrompic*  
131 function (N = 37,932 SNPs, Figure S6).

132 **Build 4: Solve minor local re-arrangements.** Runs of SNPs from Build 3 were re-assigned  
133 to new chunks flanked by recombination fractions of  $\geq 0.01$  (1 cM). Maps were reconstructed  
134 to test whether inverting chunks of  $<50$  SNPs in length and/or the deletion of chunks of  $<10$   
135 SNPs in length led to decreases in map lengths by  $\geq 1$ cM. One wrongly-orientated chunk of  
136 25 SNPs was identified on CEL15 (homologous to part of the inversion site identified on BTA28  
137 in Build 3), and the marker order was amended accordingly (reducing the map length from  
138 101.4 cM to 98.1 cM). Three chunks on the X chromosome (CEL34) shortened the map by  $\geq$   
139 1cM when inverted and were also amended accordingly, reducing the X-chromosome map by  
140 10.8 cM. The deletion of 35 individual SNPs on 14 linkage groups shortened their respective  
141 linkage maps by between 1cM and 6.3cM. A sex-averaged map of each deer linkage group was  
142 reconstructed using the *chrompic* function (N = 37,897 SNPs, Figure S7).

143 **Build 5: Determining the location of unmapped markers and resolving phasing errors.**  
144 In Builds 1 to 4, 372 SNPs in 89 chunks were removed from the analysis. To determine their  
145 likely location relative to the Build 5 map, LD was calculated between each unmapped SNP and  
146 all other SNPs in the genome to identify its most likely linkage group. The CRI-MAP *chrompic*  
147 function provides information on SNP phase (i.e. where the grandparent of origin of the allele  
148 could be determined) on chromosomes transmitted from the FID to offspring. The correlation  
149 between allelic phase was calculated for each unmapped marker and all markers within a 120  
150 SNP window around its most likely position. A total 186 SNPs in 18 chunks could be unambigu-  
151 ously mapped back to the genome; for all other markers, their most likely location was defined  
152 as the range in which the correlation of allelic phase with mapped markers was  $\geq 0.9$  (Adjusted  
153  $R^2$ ). A provisional sex-averaged map of each deer linkage group was reconstructed using the  
154 *chrompic* function (N = 38,083 SNPs). Marker orders were reversed on deer linkage groups 6,  
155 8, 16, 22 and 31 to match the orientation of the cattle genome.

156 Errors in determining the phase of alleles can lead to incorrect calling of double crossovers  
157 (i.e. two or more crossovers occurring on the same chromosome) over short map distances,  
158 leading to errors in local marker order. To reduce the likelihood of calling false double crossover  
159 events, runs of grandparental origin consisting of a single SNP (resulting in a false double  
160 crossover across that SNP) were recoded as missing (Figure S8) and the *chrompic* function  
161 was rerun. Of the remaining double crossovers, those occurring over distances of  $\leq 10\text{cM}$  (as  
162 measured by the distance between markers immediately flanking the double crossover) were  
163 also recoded as missing. Finally, sex-averaged and sex-specific maps of each deer linkage  
164 group were reconstructed using the *chrompic* and *map* functions (Figure 2, Figure S9).

165 **Build 6: Building a skeleton map and testing fine-scale order variations.** In Build 5, 71.6%  
166 of intra-marker distances were 0cM; therefore, a “skeleton map” was created to examine local  
167 changes in marker orders. All runs of SNPs were re-assigned to new chunks where all SNPs  
168 mapped to the same cM position; of each chunk, the most phase-informative SNP was identified  
169 from the *.loc* output from the CRI-MAP *prepare* function (N = 10,835 SNPs). The skeleton  
170 map was split into windows of 100 SNPs with an overlap of 50 SNPs, and the CRI-MAP *flips*  
171 function was used to test the likelihood of marker order changes of 2 to 5 adjacent SNPs (*flips2*  
172 to *flips5*). Rearrangements improving the map likelihood by  $>2$  would have been investigated  
173 further; however, no marker rearrangement passed this threshold and so the Build 5 map was  
174 assumed to be the most likely map order (Map provided in Table S1).

## 175 **Determining the lineage of origin of chromosome rearrangements.**

176 Lineages of origin and/or verification of potential chromosomal rearrangements was attempted  
177 by aligning SNP flanking sequences (as obtained from Brauning *et al.*, 2015) to related genome  
178 sequences using BLAST v2.4.0+ (Camacho *et al.*, 2009). ; Cattle and sheep diverged from  
179 deer  $\sim 27.31$  Mya, and diverged from each other  $\sim 24.6$  Mya (Hedges *et al.*, 2015)); therefore,  
180 rearrangements were assumed to have occurred in the lineage that differed from the other two.  
181 Alignments were made to cattle genome versions vUMD3.0 and Btau\_4.6.1 and to the sheep  
182 genome Oar\_v3.1 using default parameters in *blastn*, and the top hit was retained where  $\geq$   
183 85% of bases matched over the informative length of the SNP flanking sequence.

## 184 **Variation in recombination rate and landscape.**

185 Estimated genomic positions were calculated for each SNP based on the difference in cattle  
186 base pair position of sequential markers. At the boundaries of inversions and fusions, the base  
187 pair difference between markers was estimated assuming that map distances of 1cM were  
188 equivalent to 1 megabase (Mb). In cases of fissions, the first base pair position was estimated  
189 as the mean start position of the cattle chromosomes. Estimated genomic positions are given  
190 in Table S1. The relationship between linkage map and chromosome lengths for each sex were  
191 estimated using linear regression in R v3.3.2. To investigate intra-chromosomal variation in re-  
192 combination rates, the probability of crossing over was determined within 1 Mb windows using  
193 the estimated genomic positions. This was calculated as the sum of recombination fractions  
194  $r$  within the window; the  $r$  between the first and last SNPs and each window boundary was  
195 calculated as  $r \times N_{boundary} / N_{adjSNP}$ , where  $N_{boundary}$  is the number of bases to the window  
196 boundary and  $N_{adjSNP}$  is the number of bases to the adjacent window SNP. All deer chromo-  
197 somes are acrocentric, with the exception of the X chromosome (CEL34) and one unknown  
198 autosome (Gustavsson & Sundt, 1968), and are orientated in the same direction as the cat-  
199 tle genome, where centromeres are located at the beginning of the acrocentric chromosomes  
200 (Band *et al.*, 2000; Ma *et al.*, 2015). Here, we assumed the position of the centromere was at the  
201 start of the chromosome. Variation in crossover probability relative to telomeric and centromeric  
202 regions was modelled using a loess smoothing function.

**Table 1:** Synteny between the cattle and deer genomes. Large-scale fissions and fusions are informed by Slate et al (Slate *et al.*, 2002) and confirmed in this study through sequence alignment. The estimated length is calculated based on homologous SNP positions on the cattle genome BTA vUMD 3.0.

Deer Linkage Group (CEL)	Cattle Chr (BTA)	Number of Loci	Estimated Length (Mb)	Sex-averaged map length (cM)	Male map length (cM)	Female map length (cM)	Notes
1	15	1158	82.7	88.7	75.2	96.7	
2	29	663	50.3	55.4	51.6	57.5	
3	5	885	57.7	63.8	56.5	67.8	Fission from CEL22 in deer lineage.
4	18	971	65.2	81.3	72.5	85.9	
5	17, 19	2039	137.9	126.8	119.7	130.8	Fusion of BTA17 & BTA19 in deer lineage.
6	6	723	52.6	59.6	52.8	63.5	Fission from CEL17 in deer lineage.
7	23	660	51.7	64.0	60.6	65.7	
8	2	860	58.0	62.1	54.4	66.7	Fission from CEL33 in deer lineage.
9	7	1690	111.8	109.4	96.7	116.7	
10	25	580	42.7	55.3	49.1	59.2	
11	11	1547	107.1	101.3	81.7	112.1	
12	10	1486	102.1	104.2	94.0	110.0	
13	21	986	69.8	76.3	61.9	84.3	
14	16	1113	82.2	85.0	79.4	88.2	
15	26, 28	1357	96.4	96.4	79.2	105.9	Fission BTA26 & BTA28 cattle lineage. ~13Mb inversion in deer lineage and ~1.5Mb inversion in cattle lineage on segment syntenic with BTA28.
16	8	674	47.0	54.8	52.8	56.2	Fission from CEL29 in deer lineage.
17	6	1059	68.3	67.0	59.0	71.5	Fission from CEL6 in deer lineage.
18	4	1831	120.7	108.0	98.8	113.3	
19	1	1476	101.9	99.3	85.1	107.3	Fission from CEL31, then ~36Mb inversion in deer lineage.
20	3	1810	118.6	112.9	95.6	122.9	
21	14	1236	84.1	85.5	69.7	94.6	
22	5	882	62.3	65.2	55.2	71.1	Fission from CEL3 in deer lineage.
23	13	1200	83.3	95.1	84.6	101.1	~5.9Mb inversion in cattle lineage.
24	22	885	61.3	69.7	59.1	75.9	
25	20	1066	72.1	76.0	66.9	80.6	
26	9	633	41.7	51.7	50.9	52.2	Fission from CEL28 in deer lineage.
27	24	886	62.5	62.2	47.8	70.7	
28	9	938	65.5	64.7	60.3	67.2	Fission from CEL26 in deer lineage.
29	8	969	67.2	65.9	59.2	69.4	Fission from CEL16 in deer lineage.
30	12	1220	86.2	86.9	74.4	94.0	
31	1	892	57.7	59.1	53.3	62.3	Fission from CEL19 in deer lineage.
32	27	623	46.7	56.7	52.5	59.2	
33	2	1220	80.4	80.8	70.3	86.9	Fission from CEL8 in deer lineage.
34	X	1865	148.2	148.7	40.0	138.9	Three translocations (two in deer, one in cattle) and one ~ 18Mb inversion in cattle lineage; see Figure S5.
All		38083	2644.1	2739.7	2320.8	2906.3	Male and female autosomal maps of 2280.8 cM and 2767.4 cM, respectively.

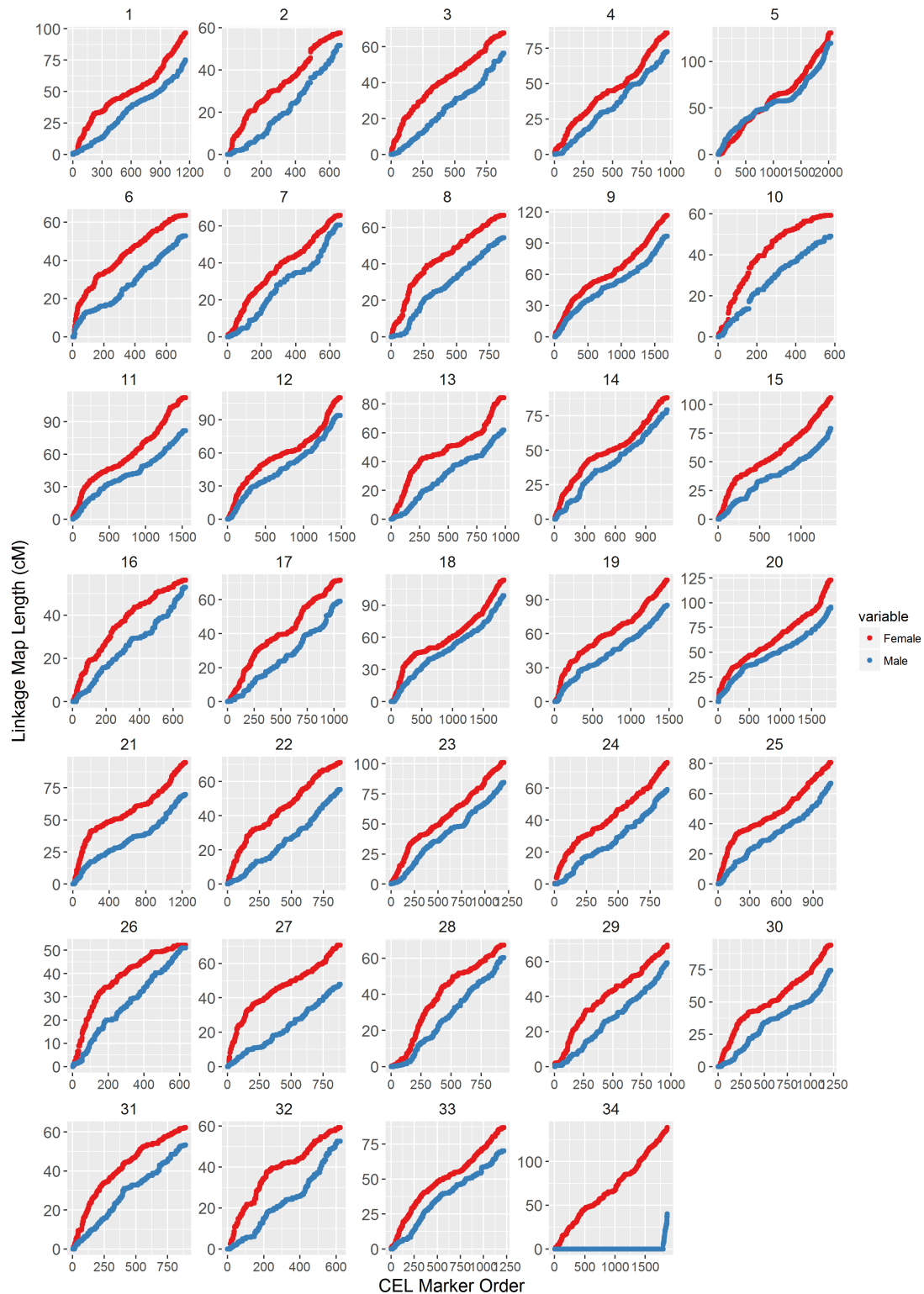


**Figure 2:** Sex-specific linkage maps for *Cervus elaphus* (CEL) linkage groups after Build 5. Map data is provided in Tables 1 and Table S1.

## 203 Results

### 204 Linkage map.

205 The predicted sex-averaged red deer linkage map contained 38,083 SNP markers over 33 au-  
206 tosome and the X chromosome (Full map provided in Table S1), and had a sex-averaged  
207 length of 2739.7cM (Table 1). A total of 71.6% of intra-marker recombination fractions were  
208 zero; a skeleton map of 10,835 SNPs separated by at least one meiotic crossover was also  
209 characterised (Table S1). The female autosomal map was 1.21 times longer than in males  
210 (2767.4 cM and 2280.8 cM, respectively, Table 1). In the autosomes, we observed six chromo-  
211 somal fissions, one fusion and two large and formerly uncharacterised inversions occurring in  
212 the deer lineage (Table 1, Figure 3). Otherwise, the deer map order generally conformed to the  
213 cattle map order. The X chromosome had undergone the most differentiation from cattle, with  
214 evidence of three translocations, including two in the deer lineage and one in the cattle lineage,  
215 and one inversion in the cattle lineage (Figure S5, Table S2). The approximate positions of 90  
216 unmapped markers are provided in Table S3.

### 217 Variation in recombination rate.

218 There was a linear relationship between estimated chromosome length and sex-averaged link-  
219 age map lengths (Adjusted  $R^2 = 0.961$ , Figure 4A). Smaller chromosomes had higher recom-  
220 bination rates (cM/Mb, Adjusted  $R^2 = 0.387$ , Figure 4B), which is likely to be a result of obligate  
221 crossing over. Female linkage maps were consistently longer than male linkage maps across  
222 all autosomes (Adjusted  $R^2 = 0.907$ , Figures S10) and correlations between estimated map  
223 lengths and linkage map lengths were similar in males and females (Adjusted  $R^2 = 0.910$  and  
224  $0.954$ , respectively; Figure S11). In order to ensure that sex-differences in map lengths are  
225 not due to the over-representation of female meioses in the dataset, maps were reconstructed  
226 for ten subsets of 483 male and 483 female FIDs randomly sampled with replacement from  
227 the dataset; there was no significant difference between the true and sampled map lengths in  
228 males and females (Figure S13), suggesting accuracy in sex-specific map lengths. Fine-scale  
229 variation in recombination rate across chromosomes was calculated in 1Mb windows across  
230 the genome; recombination rate was considerably higher in females in the first ~20% of the

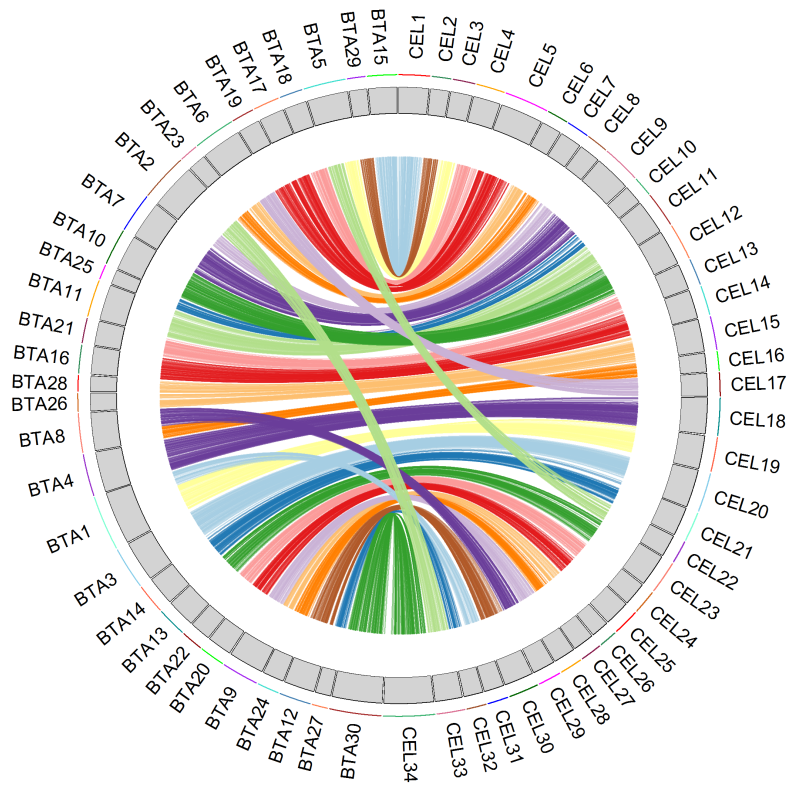


**Figure 3:** Comparison of marker positions on red deer linkage groups (right, ordered and prefixed CEL) and their predicted positions on cattle chromosomes (left, prefixed BTA). Data is shown for a sample of 2,000 SNPs. Large-scale rearrangement information and map data is provided in Tables 1 and Table S1, respectively. Plot was produced using the R package RCircos v1.1.3 (Zhang *et al.*, 2013) in R v3.3.2

231 chromosome, where the centromere is likely to be situated (Figure 5). This effect was consis-  
232 tent across nearly all autosomes, with the exception of CEL5 and CEL28 (Figure S12). Male  
233 and female recombination rates were not significantly different across the rest of the chro-  
234 mosome, although male recombination was marginally higher than females in sub-telomeric  
235 regions where the centromere was absent (Figure 5).

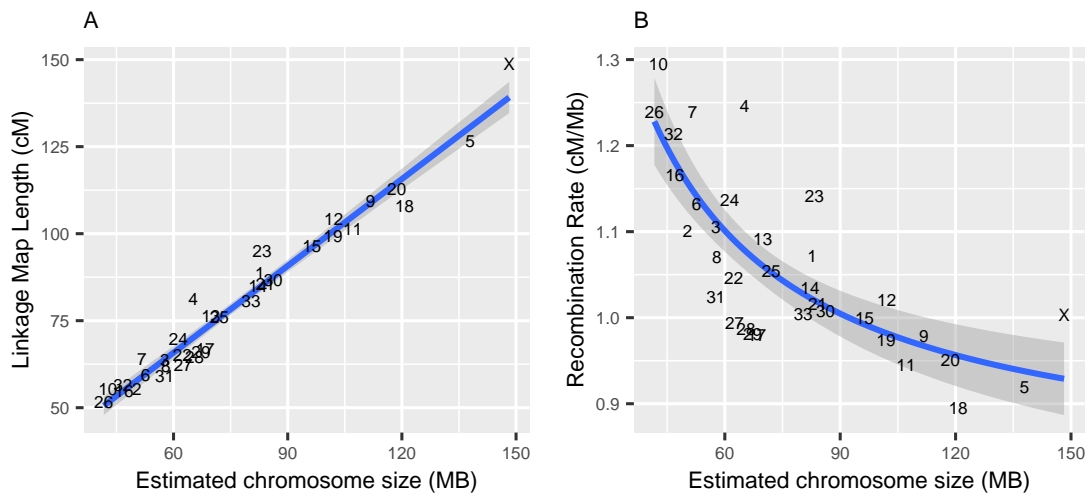


**Figure 4:** Broad-scale variation in recombination rate, showing correlations between (A) sex-averaged linkage map length (cM) and estimated chromosome length (Mb) and (B) estimated chromosome length (Mb) and chromosomal recombination rate (cM/Mb). Points are chromosome numbers, and lines and the grey-shaded areas indicate the regression slopes and standard errors, respectively.

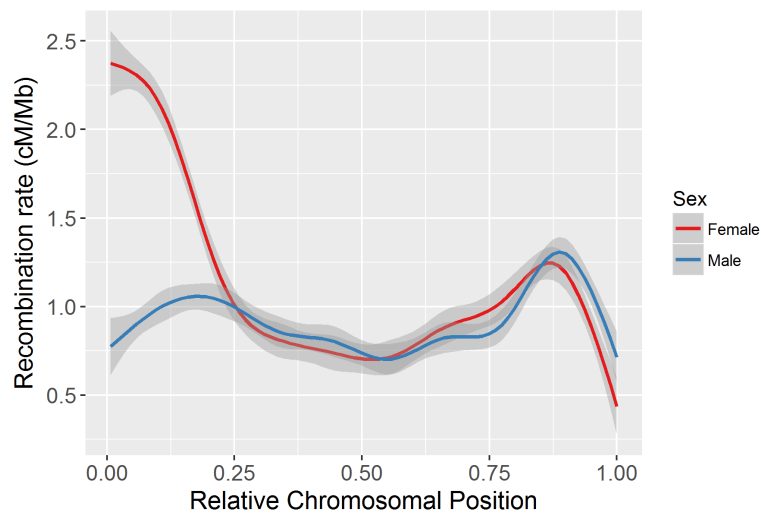


**Figure 5:** Loess smoothed splines of recombination rates across 33 autosomes for males and females. With the exception of one unknown linkage group, all chromosomes are acrocentric with the centromere at the beginning of the chromosome. Splines for individual chromosomes are shown in Figure S12

## 236 Discussion

237 **Utility of the red deer linkage map.** In this study, we constructed a predicted linkage map  
238 of 38,083 SNPs and a skeleton map of 10,835 SNPs for a wild population of red deer. The  
239 predicted map included 98.8% of polymorphic SNPs within this population. Whilst several large-  
240 scale rearrangements were identified in the red deer lineage (Table 1, Figure 3), marker orders  
241 generally showed strong concordance to the cattle genome order. We are confident that the  
242 maps presented here are highly accurate for the purposes of genetic analyses outlined in the  
243 introduction; however, we also acknowledge that some errors are likely to be present. The  
244 limited number of meioses characterised means that we cannot guarantee a correct marker  
245 order on the predicted map at the same centiMorgan map positions, meaning that some small  
246 rearrangements may be undetected within the dataset. Furthermore, the use of the cattle  
247 genome to inform initial marker order may also introduce error in cases of genome misassembly.  
248 Considering these issues, we recommend that the deer marker order is used to verify, rather  
249 than inform any *de novo* sequence assembly in the red deer or related species.

250 **Rearrangement of the X chromosome.** The X chromosome (CEL34) showed the highest  
251 level of rearrangement, including two translocations in the deer lineage, one of which was a  
252 small region in the pseudoautosomal region (PAR) remapped to the distal end of the chromo-  
253 some (Figure S5). The X chromosome also showed a similar pattern to the autosomes in the  
254 relationship between estimated chromosome length (Mb) and linkage map length (cM, Figure  
255 4). This may seem counter-intuitive, as recombination rates in the X should be lower due to  
256 it spending one-third of its time in males, where meiotic crossovers only occurs on the PAR.  
257 However, female map lengths were generally longer, and 64% of the meioses used to inform  
258 sex-averaged maps occurred in females; furthermore, the female-specific map showed that the  
259 X conformed to the expected map length. Therefore, the linkage map length of the X is as  
260 expected, and not inflated due to mapping errors. Nevertheless, we acknowledge again that  
261 mapping errors may be present on the X, particularly given that fewer informative meioses can  
262 be detected on in non-PAR regions.

263 **Sexual dimorphism in recombination landscape.** Females had considerably higher recom-  
264 bination rates in pericentromeric regions, resulting in female-biased recombination rates overall;

265 recombination rates along the rest of the chromosome were similar in both sexes and lowest  
266 at the closest proximity to the telomere (Figure 5). Identifying female-biased heterochiasmy is  
267 not necessarily unusual, as recombination rates in placental mammals are generally higher in  
268 females (Lenormand & Dutheil, 2005), and are hypothesised to protect against aneuploidy (i.e.  
269 non-disjunction) after long periods of meiotic arrest (Morelli & Cohen, 2005; Coop & Przeworski,  
270 2007; Nagaoka *et al.*, 2012). However, the pattern of heterochiasmy observed in this dataset  
271 is striking for several reasons. First, our findings are distinct from the other ruminants, namely  
272 cattle and sheep, which both exhibit male-biased heterochiasmy driven by elevated male re-  
273 combination rates in sub-telomeric regions, with similar male and female recombination rates  
274 in pericentromeric regions (Ma *et al.*, 2015; Johnston *et al.*, 2016). Second, mammal studies  
275 to date show markedly increased male recombination rates at the sub-telomere, even if female  
276 recombination rates are higher overall (e.g. in humans and mice); this is not observed in the  
277 red deer map. Third, whilst female recombination rates tend to be relatively higher in pericen-  
278 tromeric regions in many species, they are generally suppressed in very close proximity the  
279 centromere (Brandvain & Coop, 2012); evidence from human studies suggests that increased  
280 centromeric recombination can result in aneuploid gametes (Lamb *et al.*, 2005).

281 At present, the mechanisms and biological significance of elevated female recombination rates  
282 around the centromere in female deer remains unclear, although ideas have been proposed to  
283 explain variation in sex differences more generally. One proposition is selection on gametes  
284 at the haploid stage in males may vary relative to the strength of sperm competition, favour-  
285 ing particular rates of recombination (Lenormand & Dutheil, 2005; Mank, 2009). In addition,  
286 increased telomeric recombination may allow more rapid sperm turnover during gametogen-  
287 esis (Tankimanova *et al.*, 2004). Both of these ideas this may explain the difference in pat-  
288 terns observed between sheep and cattle (strong and moderate rates of sperm competition,  
289 respectively) with deer, which have relatively low sperm competition in the rut (Clutton-Brock  
290 *et al.*, 1982). However, support for this sperm competition hypothesis is only weakly supported  
291 (Trivers, 1988; Mank, 2009) and still fails to explain increased centromeric recombination in fe-  
292 males. Other explanations may relate to reduced crossover interference at the centromere in  
293 females (Fledel-Alon *et al.*, 2009) and increased recombination rates between female meiotic  
294 drive elements and the centromere (Brandvain & Coop, 2012), although neither appear to the  
295 explain consistency of sex-differences and elevated female recombination across all acrocentric  
296 chromosomes (Figure S12). Regardless, more empirical investigation is required to elucidate  
297 the specific drivers of sex differences in recombination rate and elevated centromeric recom-

298 bination in this system. Future work will investigate the heritability and genetic architecture  
299 of recombination rate at an individual level and investigate the potential role of recombination  
300 modifiers in driving rate variation within this species.

## 301 **Acknowledgements**

302 We thank T. Clutton-Brock, F. Guinness, S. Albon, A. Morris, S. Morris, M. Baker and many  
303 others for collecting field data and DNA samples and their important contributions to the long-  
304 term Rum deer project. Discussions with Camillo Bérénos & Judith Risse aided the study in its  
305 early stages; we also appreciate feedback from Graham Coop, Loukas Theodosiou, Annaliese  
306 Mason and Yaniv Brandvain on interpreting some of the results. We thank Scottish Natural  
307 Heritage for permission to work on the Isle of Rum National Nature Reserve, and Wellcome  
308 Trust Clinical Research Facility Genetics Core in Edinburgh for performing the genotyping. This  
309 work has made extensive use of the resources provided by the University of Edinburgh Compute  
310 and Data Facility (<http://www.ecdf.ed.ac.uk/>). The long-term project Rum deer is funded by  
311 the UK Natural Environment Research Council, and SNP genotyping and current work were  
312 supported by a European Research Council Advanced Grant to J.M.P.

## 313 **Author Contributions**

314 J.M.P and J.H. organised the collection of samples. P.A.E. and J.H. conducted DNA sample  
315 extraction and genotyping. J.M.P. and S.E.J. designed the study. S.E.J. analysed the data and  
316 wrote the paper. All authors contributed to revisions.

## 317 **References**

- 318 Aulchenko YS, Ripke S, Isaacs A, van Duijn CM (2007) GenABEL: an R library for genome-wide  
319 association analysis. *Bioinformatics*, **23**, 1294–1296.
- 320 Band MR, Larson JH, Rebeiz M, *et al.* (2000) An ordered comparative map of the cattle and  
321 human genomes. *Genome Res.*, **10**, 1359–1368.

- 322 Bérénos C, Ellis PA, Pilkington JG, Lee SH, Gratten J, Pemberton JM (2015) Heterogeneity of  
323 genetic architecture of body size traits in a free-living population. *Mol. Ecol.*, **24**, 1810–1830.
- 324 Bradbury IR, Hubert S, Higgins B, *et al.* (2013) Genomic islands of divergence and their con-  
325 sequences for the resolution of spatial structure in an exploited marine fish. *Evol. Appl.*, **6**,  
326 450–461.
- 327 Brandvain Y, Coop G (2012) Scrambling eggs: meiotic drive and the evolution of female recom-  
328 bination rates. *Genetics*, **190**, 709–23.
- 329 Brauning R, Fisher PJ, McCulloch AF, *et al.* (2015) Utilization of high throughput genome se-  
330 quencing technology for large scale single nucleotide polymorphism discovery in red deer  
331 and canadian elk. *bioRxiv*.
- 332 Brieuc MSO, Waters CD, Seeb JE, Naish KA (2014) A dense linkage map for chinook salmon  
333 (*Oncorhynchus tshawytscha*) reveals variable chromosomal divergence after an ancestral  
334 whole genome duplication event. *G3: Genes/Genomes/Genetics*, **4**, 447–460.
- 335 Camacho C, Coulouris G, Avagyan V, *et al.* (2009) BLAST+: architecture and applications. *BMC*  
336 *Bioinf.*, **10**, 1–9.
- 337 Clutton-Brock T, Guinness F, Albon S (1982) *Red Deer. Behaviour and Ecology of Two Sexes*.  
338 University of Chicago Press.
- 339 Coop G, Przeworski M (2007) An evolutionary view of human recombination. *Nat Rev Genet*,  
340 **8**, 23–34.
- 341 Ellegren H (2014) Genome sequencing and population genomics in non-model organisms.  
342 *Trends Ecol. Evol.*, **29**, 51–63.
- 343 Fierst JL (2015) Using linkage maps to correct and scaffold de novo genome assemblies: meth-  
344 ods, challenges, and computational tools. *Front. Genet.*, **6**, 220.
- 345 Fledel-Alon A, Wilson DJ, Broman K, *et al.* (2009) Broad-scale recombination patterns underly-  
346 ing proper disjunction in humans. *PLoS Genet.*, **5**, e1000658.
- 347 Fountain T, Ravinet M, Naylor R, Reinhardt K, Butlin RK (2016) A linkage map and QTL analysis  
348 for pyrethroid resistance in the bed bug *Cimex lectularius*. *G3: Genes/Genomes/Genetics*, **6**,  
349 4059–4066.

- 350 Frantz AC, Pourtois JT, Heuertz M, *et al.* (2006) Genetic structure and assignment tests demon-  
351 strate illegal translocation of red deer (*Cervus elaphus*) into a continuous population. *Mol.*  
352 *Ecol.*, **15**, 3191–3203.
- 353 Green P, Falls K, Crooks S (1990) *Documentation for CRIMAP, version 2.4*. Washington Uni-  
354 versity School of Medicine.
- 355 Gustavsson I, Sundt CO (1968) Karyotypes in five species of deer (*Alces alces* L., *Capreolus*  
356 *capreolus* L., *Cervus elaphus* L., *Cervus nippon nippon* temm. and *Dama dama* L.). *Hereditas*,  
357 **60**, 233–248.
- 358 Hedges SB, Marin J, Suleski M, Paymer M, Kumar S (2015) Tree of life reveals clock-like spe-  
359 ciation and diversification. *Mol. Biol. Evol.*, **32**, 835–845.
- 360 Huisman J (2017) Pedigree reconstruction for SNP data: parentage assignment, sibship clus-  
361 tering and beyond. *Mol. Ecol. Resour.*, **In revision**.
- 362 Huisman J, Kruuk LEB, Ellis PA, Clutton-Brock T, Pemberton JM (2016) Inbreeding depression  
363 across the lifespan in a wild mammal population. *Proc. Natl. Acad. Sci. U.S.A.*, **113**, 3585–  
364 3590.
- 365 Johnston SE, Bérénos C, Slate J, Pemberton JM (2016) Conserved Genetic Architecture Un-  
366 derlying Individual Recombination Rate Variation in a Wild Population of Soay Sheep (*Ovis*  
367 *aries*). *Genetics*.
- 368 Kardos M, Taylor HR, Ellegren H, Luikart G, Allendorf FW (2016) Genomics advances the study  
369 of inbreeding depression in the wild. *Evol. Appl.*, **9**, 1205–1218.
- 370 Kawakami T, Smeds L, Backström N, *et al.* (2014) A high-density linkage map enables a  
371 second-generation collared flycatcher genome assembly and reveals the patterns of avian  
372 recombination rate variation and chromosomal evolution. *Mol. Ecol.*, **23**, 4035–4058.
- 373 Kruuk LEB, Slate J, Pemberton JM, Brotherstone S, Guinness F, Clutton-Brock T (2002) Antler  
374 size in red deer: heritability and selection but no evolution. *Evolution*, **56**, 1683–1695.
- 375 Lamb NE, Sherman SL, Hassold TJ (2005) Effect of meiotic recombination on the production  
376 of aneuploid gametes in humans. *Cytogenet. Genome Res.*, **111**, 250–255.
- 377 Lander ES, Schork NJ (1994) Genetic dissection of complex traits. *Science*, **265**, 5181.

- 378 Leitwein M, Guinand B, Pouzadoux J, Desmarais E, Berrebi P, Gagnaire PA (2016) A dense  
379 brown trout (*Salmo trutta*) linkage map reveals recent chromosomal rearrangements in the  
380 salmo genus and the impact of selection on linked neutral diversity. *bioRxiv*.
- 381 Lenormand T, Dutheil J (2005) Recombination difference between sexes: a role for haploid  
382 selection. *PLoS Biol.*, **3**, e63.
- 383 Ma L, O'Connell JR, VanRaden PM, *et al.* (2015) Cattle Sex-Specific Recombination and Ge-  
384 netic Control from a Large Pedigree Analysis. *PLoS Genet.*, **11**, e1005387.
- 385 Mank JE (2009) The evolution of heterochiasmy: the role of sexual selection and sperm com-  
386 petition in determining sex-specific recombination rates in eutherian mammals. *Genet. Res.*,  
387 **91**, 355–363.
- 388 McKinney GJ, Seeb LW, Larson WA, *et al.* (2016) An integrated linkage map reveals candidate  
389 genes underlying adaptive variation in chinook salmon (*Oncorhynchus tshawytscha*). *Mol.*  
390 *Ecol. Resour.*, **16**, 769–783.
- 391 Morelli MA, Cohen PE (2005) Not all germ cells are created equal: Aspects of sexual dimor-  
392 phism in mammalian meiosis. *Reproduction*, **130**, 761–781.
- 393 Nagaoka SI, Hassold TJ, Hunt PA (2012) Human aneuploidy: mechanisms and new insights  
394 into an age-old problem. *Nat. Rev. Genet.*, **13**, 493–504.
- 395 Rastas P, Calboli FCF, Guo B, Shikano T, Merilä J (2016) Construction of ultradense linkage  
396 maps with Lep-MAP2: Stickleback F2 recombinant crosses as an example. *Genome Biol.*  
397 *Evol.*, **8**, 78–93.
- 398 Senn HV, Pemberton JM (2009) Variable extent of hybridization between invasive sika (*Cervus*  
399 *nippon*) and native red deer (*C. elaphus*) in a small geographical area. *Mol. Ecol.*, **18**, 862–  
400 876.
- 401 Slate J, Van Stijn TC, Anderson RM, *et al.* (2002) A deer (subfamily *Cervinae*) genetic linkage  
402 map and the evolution of ruminant genomes. *Genetics*, **160**, 1587–1597.
- 403 Sturtevant AH (1913) The linear arrangement of six sex-linked factors in *Drosophila*, as shown  
404 by their mode of association. *J. Exp. Zool.*, **14**, 43–59.
- 405 Tankimanova M, Hultén Ma, Tease C (2004) The initiation of homologous chromosome synapsis  
406 in mouse fetal oocytes is not directly driven by centromere and telomere clustering in the  
407 bouquet. *Cytogenet. Genome Res.*, **105**, 172–181.

- 408 Trivers R (1988) Sex differences in rates of recombination and sexual selection. In *The evolution*  
409 *of sex*. (edited by R Michod, B Levin), pp. 270–286. Sinauer Press., Sunderland, MA, USA.
- 410 Zhang H, Meltzer P, Davis S (2013) RCircos: an R package for Circos 2D track plots. *BMC*  
411 *Bioinf.*, **14**, 244.